Fluctuation growth and spinodal decomposition in heavy ion reactions

David H. Boal and James N. Glosli
Department of Physics, Simon Fraser University, Burnaby, British Columbia, Canada V5A 1S6
(Received 5 March 1990)

The liquid/vapor phase diagram of a Hamiltonian-based model for nuclear dynamics (quasiparticle dynamics) is determined. Finite-size effects in the coexistence region and the time scale for fluctuation growth associated with spinodal decomposition are quantitatively investigated. For finite nuclei, no direct link is found between the phase diagram and either the rate of fluctuation growth or its density dependence.

The phase diagram of neutral nuclear matter is known to possess a liquid/vapor phase transition.[1,2] Bertsch and Siemens[3] have pointed out that the mechanical instability region of the phase diagram may play a role in fragment formation during heavy-ion collisions. Within the mechanical instability region, defined by the spinodal curves $\partial P/\partial\rho < 0$ at constant temperature or constant entropy, a homogeneous system is unstable against fluctuation growth and separates into distinct liquid and vapor components.

Fluctuation growth in infinite Fermi fluids at low temperature has been treated analytically.[4] Computer simulations of reaction trajectories in the phase-transition region have been explored for (atomic) argon droplets,[5] Boltzmann nucleons,[6] and a number of approximate fermion models.[7,8] In the simulations there appears to be a minimum density below which an evolving nuclear system irreversibly breaks apart. However, no link between this density and corresponding thermodynamic properties has been established.

In this paper, the quasiparticle dynamics model[9] (QPD hereafter) is used to investigate fluctuation growth in infinite systems and fragmentation in nuclear reactions. QPD is a many-body theory in which each nucleon is represented by a quasiparticle with a fixed-width Gaussian density distribution in phase space. In the model, the phase-space coordinates of the quasiparticle $\mathbf{R}_i$ and $\mathbf{P}_i$ corresponding to the expectations $\langle r\rangle_i$ and $\langle p\rangle_i$ of the Gaussian distributions are propagated by Hamilton's equations and a stochastic collision term between nucleons. The quasiparticle Hamiltonian consists of the Coulomb potential, a nuclear potential, and a momentum-dependent "Pauli" potential, the latter representing the energetics of fermions arising from the Pauli exclusion principle. As a result of the Pauli potential, ground-state nuclei in QPD have nonzero $\langle p^2\rangle$. The collision term conserves linear and angular momentum, as well as energy, but is stochastic in that the scattering point is randomly chosen.[9] QPD has been used as a transport model to investigate inclusive spectra characteristics in nuclear reactions.[10]

First, we wish to establish that an infinite system obeying the QPD Hamiltonian possesses a similar phase diagram to what is found in other nuclear matter models.[1-4,7,11] We determine the QPD phase diagram by calculating the specific heat at constant volume C_V with the traditional Metropolis Monte Carlo procedure[12] and the fluctuation-dissipation theorem. At each T-ρ point, a simulation is performed for up to six finite systems of A nucleons ($A=16$, 32, 64, 128, 256, and 512) placed in a box with periodic boundary conditions. The size of the box is determined by the density ρ of interest. The system is isospin symmetric, but has no Coulomb interaction. Conditional moves are made on each quasiparticle's phase-space coordinate, and sample configurations are stored after enough moves have been accepted that the successive samples are largely uncorrelated. Typically 8000 samples are used per T-ρ point, although near the critical point 12000 samples are generated per point.

A pseudotransition temperature is associated with the temperature $T_m(\rho,A)$ at which $C_V(T,\rho,A)$ of the finite system is a maximum. By considering the surface term in the free energy, the size dependence of $T_m(\rho,A)$ to leading order in $1/A$ can be taken to have the form

$$T_m(\rho,A)=T_t(\rho)+B(T_t,\rho)/A^{1/3}, \tag{1}$$

where $B(T_t,\rho)$ is an unknown function of ρ and $T_t(\rho)$, the infinite system transition temperature. For each T-ρ point, $T_m(\rho,A)$ determined numerically is plotted against $A^{-1/3}$ to determine $T_t(\rho)$ by extrapolation. The constant $B(T_t,\rho)$, although not of physical interest, is also then determined.

Shown in Fig. 1 are both T_m and the estimated T_t for $A=16$-512. The curve passing near the points labeled "infinite" represents our estimate of the liquid/vapor coexistence boundary. Outside this region, the vapor phase is favored on the low-density side of the critical point, and the liquid phase is favored on the high-density side. We estimate a critical temperature of 18.5 MeV and a critical density of 0.05 fm^{-3} (or $0.3\rho_0$, where $\rho_0=0.17$ fm^{-3}), similar to values reported in other studies.[1-4,7,11] However, our results further show that nuclear systems exhibit strong finite-size effects for system sizes typical of real nuclei. In turn, this makes the observation of the transition in nuclear reactions all the more difficult. A numerical determination of the spinodal curves $\partial P/\partial p < 0$ which are contained within the coexistence region is beyond our computational capabilities. Because our phase diagram is similar to other model phase diagrams, we expect that the spinodal region will also be similar, and would correspond roughly to the $A=128$ curve in Fig. 1 for the constant en-

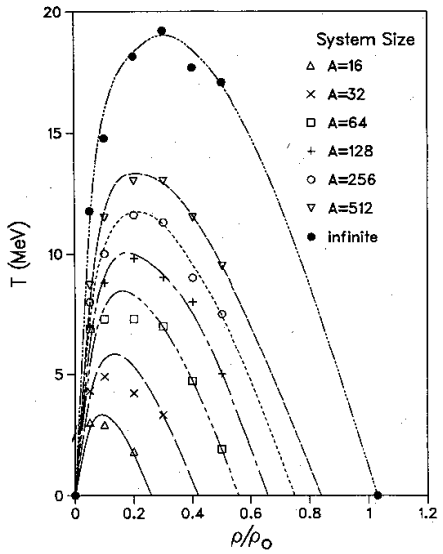

FIG. 1. Phase diagram of QPD nuclear matter as calculated by extrapolating the temperature T_m to obtain T_t of the infinite system using Eq. (1). A range of system mass A (16–512) is shown for each density. The curve passing near the "infinite" data points is our estimate of the liquid-vapor coexistence region. The density is normalized to $\rho_0 = 0.17$ fm^{-3}.

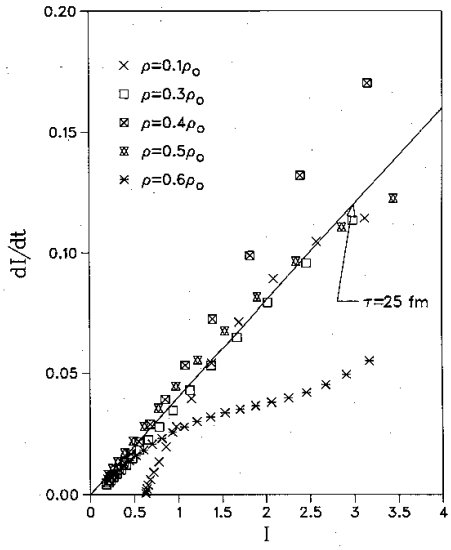

FIG. 2. Scatter plot of dI/dt vs I, where I is a measure of the fluctuations of the system (see text for definition of I). The fit to the straight line demonstrates the small time exponential growth of the fluctuations with time constant $\tau_f = 25$ fm/c.

tropy spinodal (see Refs. 1–4, 7, and 11 for comparison).

We next consider fluctuation growth in homogeneous matter. A homogeneous ground state at fixed density can be found numerically by minimizing the energy, subject to the constraint that the fluctuations $\langle\rho^2\rangle - \langle\rho\rangle^2$ are a minimum. This is accomplished by using a Lagrange multiplier method to find the minimum energy at fixed $\langle\rho^2\rangle$, where the associated multiplier is chosen such that $\langle\rho^2\rangle$ is a minimum. Periodic boundary conditions are enforced, and the quasiparticles are driven to their ground-state configurations using a set of damped Hamilton's equations as in Ref. 9. The homogeneity constraint is then removed and the system is allowed to evolve. A measure of spatial fluctuations is the quantity $I = \langle\nabla^2\rho\rangle / \langle\nabla^2\rho_1\rangle$, which compares the fluctuations of the system to those of a single isolated quasiparticle. The density distribution of a single isolated quasiparticle ρ_1 is a fixed-width Gaussian form.[9] The expectation is defined by

$$\langle\nabla^2 f\rangle \equiv \int (\nabla^2 f) f(r) d^3r \Big/ \int f(r) d^3r \, .$$

Figure 2 shows a scatter plot of dI/dt vs I for a number of different initial densities. The data are clustered about a single straight line of the form $I(t) \approx \exp(t/\tau_f)$ with $\tau_f = 25$ fm/c. This time constant indicates the rate at which clusters grow in the instability region. The fluctuation growth rate is most reliably calculated at early times (small I) before the finite box size and quasiparticle width limit the maximum size of the systems' vapor phase. These effects are at least partially responsible for the large I behavior in Fig. 2 at $\rho/\rho_0 > 0.6$. The stochastic collision term in the QPD model is not included in the calculations shown in Fig. 2.

Now we examine the time evolution and breakup of excited nuclei, choosing ^{108}Ag as an example. We excite the nuclei in one of two ways. In the first method a random radial component is added to each ground-state quasiparticle momentum $\mathbf{P}_i$ to generate a new momentum $\mathbf{P}_i' = \mathbf{P}_i + \Delta\mathbf{R}_i$ where R_i is a unit vector along the direction from the nuclear center of mass to the position of the ith particle and the Δ's are uniformly distributed random variables in the interval (ω_1, ω_2). This procedure generates radially excited states of low entropy. The second method randomizes the direction of the ground-state momentum vectors: $\mathbf{P}_{i\alpha}' = S_{i\alpha}\mathbf{P}_{i\alpha}$, where $\alpha = x$, y, or z and the S_i's are random scale factors which are distributed uniformly in the interval $(-\omega, \omega)$. The excited states of this procedure have high entropy but little initial radial expansion. For either method, values for ω are chosen so that a set of several thousand different excited states contains a sample of at least a hundred states which have an excitation energy per nucleon E^*/A within 0.5 MeV of the desired mean.

Each of the states in this collection is then allowed to evolve for several hundred fm/c using QPD including stochastic collisions. We use the average central density $\langle\rho\rangle_c$ and central fluctuations $\langle\rho^2\rangle_c - \langle\rho\rangle_c^2$ as observables. The $\langle\cdots\rangle_c$ denotes both a spatial average over a sphere of radius 4 fm centered on the center of mass and an ensemble average over the 100 events in each sample. The time dependence of $\langle\rho\rangle_c$ is shown in Fig. 3 for a variety of initial excitations. In the upper plot the results for the radial excitation are shown for mean $E^*/A = 2$, 6, and 8 MeV.

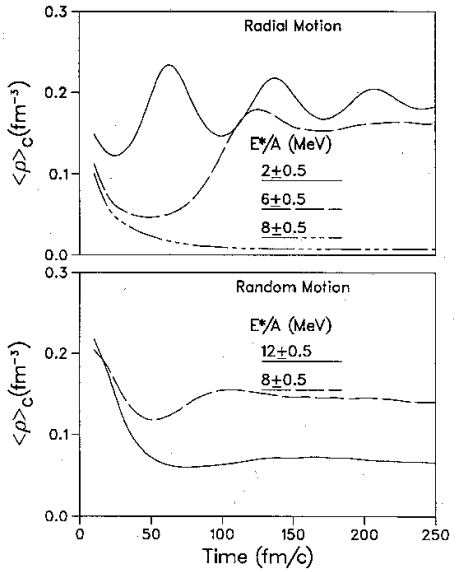

FIG. 3. The time dependence of the average central density ($\langle\rho\rangle_c$) of excited ^{108}Ag nuclei. The upper diagram illustrates the behavior for a radially outward directed excitation and the lower diagram illustrates the behavior for a much more random initial excitation.

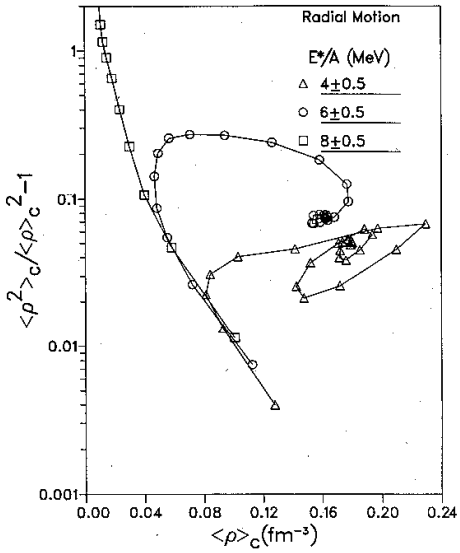

FIG. 4. Trajectories of the radially excited ^{108}Ag nuclei in density-fluctuation space. The markers on the curves are separated by 10-fm/c time intervals.

For low excitation energy the system exhibits a damped oscillation about an equilibrium value of the density. The period of this oscillation is about 75 fm/c and the relaxation time constant for the decay of the motion's amplitude is $\tau_T = 110$ fm/c. At $E^*/A = 6$ MeV, the system expands with some particle loss, but then recovers to form a highly thermalized nucleus. However, at $E^*/A = 8$ MeV the system becomes unstable and the central density $\langle\rho\rangle_c$ decays exponentially with a time constant of 15–20 fm/c. In the lower part of Fig. 3 results are shown for the random excitation. The oscillations of the system are greatly suppressed, although the systems do relax. Also the systems hold together at much larger initial excitation energies, although they suffer significant particle loss. This particle loss results in a smaller nucleus and a correspondingly low value of $\langle\rho\rangle_c$, which is averaged over a 4 fm radius.

Does the onset of fluctuation growth in the low entropy sample indicate the breakup of the system? In Fig. 4, a plot is made of $(\langle\rho^2\rangle_c/\langle\rho\rangle_c^2 - 1)$ vs $\langle\rho\rangle_c$ for several ^{108}Ag radial excitations. The marks on each curve are separated by time intervals of 10 fm/c. Initially all the systems follow the same trajectory. The low-energy trajectories split off from this common trajectory to follow separate "pig tail" paths to a thermalized state. The large excitation energy system continues to expand exponentially with a time constant τ_e of 15–20 fm/c and breaks apart. It is tempting to identify τ_f and τ_e and associate fluctuation growth with the spinodal decomposition of infinite matter in the mechanical instability region. However, the initial fluctuation growth of all the radially excited systems passes through the same region of fluctuation/density space and has very similar growth rates. Further, fluctuation growth itself does not lead to nuclear fragmentation, as seen from the curves at $E^*/A = 4$ and 6 MeV. More likely, nucleon-nucleon collisions make a significant contribution to fluctuation growth and the excitation energy determines whether the system undergoes multifragmentation.

Finally, we note that the instability leading to multifragmentation of the low-entropy radially-excited systems sets in at $\langle\rho\rangle_c < 0.05$ fm^{-3} in Fig. 4. At low entropy, this isentropic spinodal line is expected[1–4,7,11] to lie closer to 0.1 fm.$^{-3}$ Hence, we do not feel that multifragmentation can be associated with the expanding system crossing the spinodal curve of infinite matter. True heavy-ion collisions are bound to produce systems which are much less uniform than our idealized system, which resembles more closely a state of expanding nuclear matter. But even for our simple system, we see that initial fluctuations, along with those generated by the collision term in the equations of motion, very likely mask the fluctuations of the mechanical instability of infinite matter.

D.H.B. wishes to thank the Natural Sciences and Engineering Research Council of Canada for financial support.

[1]G. Sauer, H. Chandra, and U. Mosel, Nucl. Phys. **A264**, 221 (1976).
[2]D. Q. Lamb, J. M. Lattimer, C. J. Pethick, and D. G. Ravenhall, Phys. Rev. Lett. **41**, 1623 (1978).
[3]G. Bertsch and P. J. Siemens, Phys. Lett. **126B**, 9 (1983).
[4]C. J. Pethick and D. G. Ravenhall, Ann. Phys. **183**, 131 (1988).
[5]A. Vincentini, G. Jacucci, and V. R. Pandharipande, Phys. Rev. C **31**, 1783 (1985).
[6]R. J. Lenk and V. R. Pandharipande, Phys. Rev. C **34**, 177 (1986).
[7]D. H. Boal and A. L. Goodman, Phys. Rev. C **33**, 1690 (1986).
[8]D. H. Boal and J. N. Glosli, Phys. Rev. C **37**, 91 (1988).
[9]D. H. Boal and J. N. Glosli, Phys. Rev. C **38**, 1870 (1988); **38**, 2621 (1988).
[10]D. H. Boal, J. N. Glosli, and C. Wicentowich, Phys. Rev. Lett. **62**, 737 (1989); Phys. Rev. C **40**, 601 (1989).
[11]B. Friedman and V. R. Pandharipande, Nucl. Phys. **A361**, 502 (1981); J. A. Lopez and P. J. Siemens, *ibid.* **431**, 728 (1984).
[12]K. Binder and D. W. Heermann, *Monte Carlo Simulation in Statistical Physics* (Springer-Verlag, Berlin, 1988); O. G. Mouritsen, *Computer Studies of Phase Transitions and Critical Phenomena* (Springer-Verlag, Berlin, 1984).